LETTERS

Modelled atmospheric temperatures and global sea levels over the past million years

Richard Bintanja[1], Roderik S.W. van de Wal[1] & Johannes Oerlemans[1]

Marine records of sediment oxygen isotope compositions show that the Earth's climate has gone through a succession of glacial and interglacial periods during the past million years. But the interpretation of the oxygen isotope records is complicated because both isotope storage in ice sheets and deep-water temperature affect the recorded isotopic composition[1–5]. Separating these two effects would require long records of either sea level or deep-ocean temperature, which are currently not available. Here we use a coupled model of the Northern Hemisphere ice sheets[6] and ocean temperatures, forced to match an oxygen isotope record for the past million years compiled from 57 globally distributed sediment cores, to quantify both contributions simultaneously. We find that the ice-sheet contribution to the variability in oxygen isotope composition varied from ten per cent in the beginning of glacial periods to sixty per cent at glacial maxima, suggesting that strong ocean cooling preceded slow ice-sheet build-up. The model yields mutually consistent time series of continental mean surface temperatures between 40 and 80° N, ice volume and global sea level. We find that during extreme glacial stages, air temperatures were 17 ± 1.8 °C lower than present, with a 120 ± 10 m sea level equivalent of continental ice present.

Marine oxygen isotope records have provided detailed information about climatic variations over the past millions of years[7]. Interpreting the fluctuations in oxygen isotope ($\delta^{18}O$ ratio) is not straightforward, however, because the signal is affected mainly by two mechanisms (aside from local hydrographical influences). The first is preferential evaporation and subsequent incorporation of the lighter oxygen isotope in ice sheets during glacial conditions, which affects the ocean's $\delta^{18}O$ value (the 'ice-sheet part'). The second mechanism is mainly related to the uptake of $\delta^{18}O$ in calcite by benthic foraminifera, which depends on local deep-water temperature at the time of crystallization of their shells[8] (the 'deep-water part'). Previous attempts to separate these two effects involved the use of independent temperature and sea-level records to estimate either the ice-sheet part[1,9] or the deep-water part[3]. Albeit with considerable uncertainty, owing mainly to local water-mass variability, these studies have yielded long (several 100,000 yr, or 100 kyr) combined records of sea level and deep-sea temperature. These showed that the glacial deep ocean was 2–3 °C colder than today, which agrees with temperatures inferred from the Mg/Ca ratio in fossil ostracodes[10].

We have tried a different approach, one that takes advantage of the fact that on glacial–interglacial timescales, the main contributors to the mean benthic oxygen isotope record—the Northern Hemisphere ice-sheet isotope content and the local deep-sea temperature—are both strongly related to Northern Hemisphere midlatitude to subpolar surface air temperature. This puts constraints on the surface air temperature, which enabled us to separate the ice-sheet and deep-water parts simultaneously and consistently, without the need to know either in advance. Based only on $\delta^{18}O$ data, our method additionally provides reconstructions of actual climate variables such as surface air temperature, global sea level and ice volume and ice isotope content.

Ideally, the reconstructions should be as generally representative as possible, which can be achieved by an appropriate choice of input $\delta^{18}O$ record. Many long records of benthic $\delta^{18}O$ exist today, all carrying global information, but superimposed on their global signal is the unknown effect of local hydrographical effects[5]. This variability would introduce unfavourable uncertainty in the reconstructions. For this reason, we selected a recently developed benthic $\delta^{18}O$ stack based on 57 globally distributed records[11], to drive our ice-sheet–ocean-temperature model (results for two individual records are shown in the Supplementary Information). In this stack, we assume

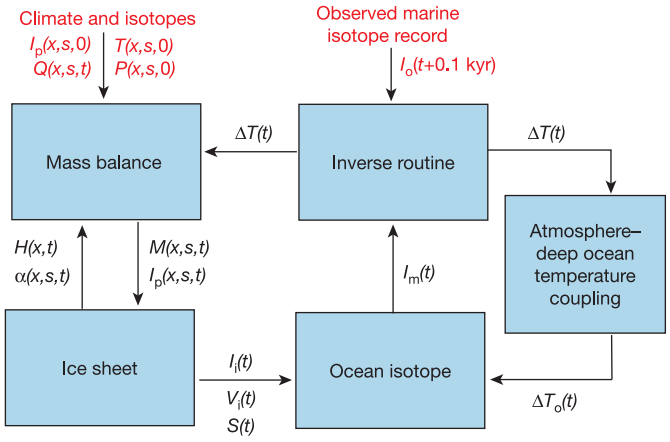

Figure 1 | Schematic outline of the inverse procedure. The routine calculates a mean surface air temperature anomaly (ΔT) based on the difference between the modelled marine isotope value ($I_m(t)$) and the observed value 0.1 kyr later ($I_o(t + 0.1\ \mathrm{kyr})$). The value of ΔT feeds into two physical systems: (1) the ice-sheet and mass-balance module to the left and (2) the atmosphere–deep ocean temperature coupling module to the right. The mass-balance module calculates spatially (x), seasonally (s) and temporally (t) varying fields of surface mass balance (M) and isotope content of precipitation (I_p) using initial, present-day (0) fields of I_p, surface air temperature (T) and precipitation (P) and temporally varying orbitally induced insolation (Q). M and I_p are used by the ice-sheet module to calculate new distributions of ice-sheet surface height (H) and surface albedo (α), which feed back into the mass balance routine. The ice-sheet routine determines the mean ice-sheet isotope content (I_i), the ice-sheet volume (V_i) and global sea level (S). These values, together with the deep-ocean temperature (ΔT_o), are used by the ocean routine to evaluate the marine isotope value (I_m) that feeds into the inverse routine. This procedure yields mutually consistent time series of ΔT, ΔT_o, V_i, S, and I_i. Observed (input) variables are in red, modelled ones in black.

[1]Institute for Marine and Atmospheric Research Utrecht, Utrecht University, Princetonplein 5, 3584 CC Utrecht, The Netherlands.

© 2005 Nature Publishing Group

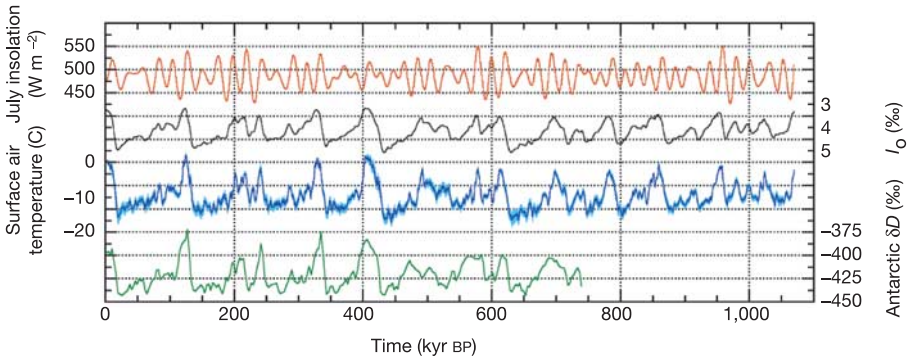

Figure 2 | 1,070-kyr time series of reconstructed Northern Hemisphere surface air temperature. Also shown are July insolation at 65° N (red), the input marine oxygen isotope stack[11] (black), modelled surface air temperature deviation from present (mean over the continents between 40° and 80° N) (blue), and Antarctic δD (ref. 14) (green). Insolation, $\delta^{18}O$ and temperature are presented on the isotope stack timescale[11], while δD is given on its own timescale[14]. The error envelope for the temperature curve represents the 1σ equivalent confidence limit derived from sensitivity tests (see Methods).

that local influences have averaged out, making it the best globally representative benthic $\delta^{18}O$ record currently available.

To separate this mean $\delta^{18}O$ signal into an ice-sheet part and a deep-water part, we used an 'inverse' technique, visualized in Fig. 1, which is based on a similar method proposed recently[12]. The basic concept of this technique is to let the model determine Northern Hemisphere subpolar surface air temperature—the variable that governs isotope storage in land ice (and hence its extraction from the ocean) and deep-ocean temperatures—under the stringent requirement that the input marine $\delta^{18}O$ record is accurately followed (see Methods for details). We let the model start at 1,070 kyr before present (BP), with interglacial conditions similar to today's, and run to the present. This yielded uninterrupted and internally consistent 1,070-kyr time series of surface air temperature deviation from present (mean continental value between 40° and 80° N), ice volume, global sea level, and the ice-sheet and deep-water components of the oxygen isotope signal at 0.1-kyr time intervals.

The fluctuations in reconstructed Northern Hemisphere surface air temperature closely follow those in the input oxygen isotope record (Fig. 2). In our inverse procedure, when the ocean gets isotopically heavier, air temperatures must decrease to build isotopically light ice sheets and to cool the deep ocean, the former being a comparatively slow mechanism. The input isotope signal also dictates the amplitude of the glacial–interglacial temperature changes, with the strongest variations occurring over the past 700 kyr. The modelled extreme Northern Hemisphere surface air temperatures for this period were 17 °C below present, with a 1σ error of 2.7 °C, in line with land-based proxy surface air temperature anomalies in subpolar Eurasia for the Last Glacial Maximum (LGM; 20 kyr BP) of −12 to −18 °C (ref. 13). The mean temperature over the 1,070-kyr period was calculated as 9.4 °C below present.

Particularly for the last 400 kyr, our reconstructed midlatitude–subpolar Northern Hemisphere temperature record compares favourably with the independent δD (deuterium) record of Dome C, Antarctica[14], the longest air temperature proxy record available at present (Fig. 2). This suggests a global coherence in temperature fluctuations on multi-millennium timescales, although uncertainties in the dating of both records prevent us from reliably determining possible interhemispheric phase differences. The magnitudes of glacial–interglacial temperature changes are in line with those in δD, and warmer-than-present interglacials at 400, 330 and 120 kyr BP can be seen in both records. Our approach shows that the beginnings of glacial periods are always marked by strong temperature drops[9] (maximum cooling of 4 °C kyr^{-1}), in agreement with the Antarctic δD record. The reconstructed cooling rate during the inception stage of the last glacial around 115 kyr BP also agrees with the $\delta^{18}O$-inferred temperature decrease observed in the North Greenland Ice-core Project (NGRIP) ice core, central Greenland[15]. Hence, the build-up of ice sheets following interglacials is associated with abrupt climate cooling. The glacial–interglacial Antarctic δD shift corresponds to a temperature amplitude of about 10 °C, suggesting that Northern Hemisphere glacial periods were significantly colder than the Antarctic, relative to the present[4].

The fluctuations in reconstructed sea levels follow those in the input $\delta^{18}O$ signal (Fig. 3a). During the greatest glacial extremes, sea level was 125 ± 12 m below present, with less extreme lows before 700 kyr BP. Our reconstructed sea-level record agrees well with sea-level estimates based on the 470-kyr Red Sea sediment $\delta^{18}O$ record[16], one of the longest continuous sea-level records available, in particular for the last glacial cycle (Fig. 3b), and also with sea-level data

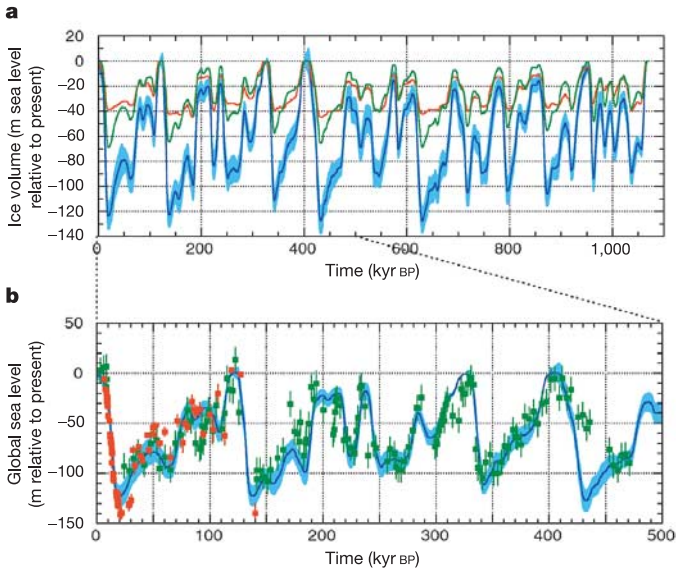

Figure 3 | Time series of past global sea level. a, Reconstructed global sea level (blue), with the 1σ confidence limit based on sensitivity tests (see Methods), and the contributions from Eurasia (red) and North America (green) in sea level equivalents. Fluctuations in global sea level are dominated by the ice sheets in North America. **b**, Reconstructed global sea level and its 1σ uncertainty (blue) compared with the 470-kyr Red Sea basin sediment $\delta^{18}O$ record[16] (green squares) and New Guinea and Barbados coral reef data for the last glacial cycle[17] (red squares). Timescales and error bars are taken from the respective studies.

© 2005 Nature Publishing Group

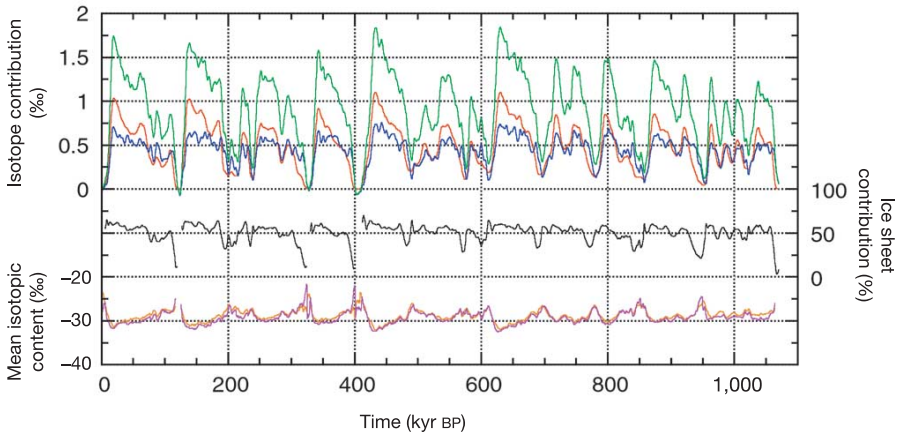

Figure 4 | Fluctuations in the various isotope signals over the 1,070-kyr period. The observed marine isotope signal with the present-day value of 3.22‰ subtracted (green) is composed of an ice-sheet contribution (red) and a deep-water temperature (blue) contribution (both simulated). The modelled relative contribution of ice sheets to the total marine isotope signal varies strongly over glacial–interglacial cycles (black). In contrast, the simulated mean isotopic content of the ice sheets in Eurasia (orange) and North America (purple) does not exhibit large fluctuations. Missing values represent periods with no significant continental ice.

deduced from fossil coral reefs[17]. Interestingly, the contribution of the Eurasian ice sheets was 40 m of sea-level equivalent at most (Fig. 3a). During the most intense glacial stages, Northern Hemisphere ice-sheet growth was thus limited to North America, which is consistent with geomorphological reconstructions[18] and modelling studies[19], at least for the LGM. When cold glacial conditions persisted for 100-kyr periods, the Laurentide ice sheet in the east of North America and the Cordilleran ice sheet in the west were able to merge into one massive ice sheet covering much of present-day Canada[19]. In Eurasia, the Fennoscandian ice sheet was consistently pushed to the western continental shelf margin, whereas very dry conditions prevented expansion to the east[20]. This geographical effect restricted further growth of the Fennoscandian ice sheet under cold glacial conditions.

The modelled mean isotopic compositions of the ice sheets only vary between −25 and −32‰ (Fig. 4, bottom). This indicates that the ice-sheet part of the marine isotope signal is governed by ice-volume fluctuations. For the Laurentide ice sheet, the LGM value of −32‰ compares very well with estimates based on $\delta^{18}O$ values in subglacial calcite of −31 ± 3‰ (ref. 8). The modelled deep-water part of the marine $\delta^{18}O$ signal exhibits a rapid increase at the beginning of glacials (Fig. 4, top), indicative of strong ocean cooling (2 to 2.5 °C) preceding ice-sheet build-up. This finding is consistent with sea surface temperature estimates based on other North Atlantic sediment cores[21], and with strong cooling of the surface air as indicated by ice-core temperature proxies[14,15] (Fig. 2). Enhanced storage of light isotopes in the expanding ice sheets causes the ice-sheet part of the $\delta^{18}O$ signal to increase steadily towards glacial extremes, followed by a sharp decline during deglaciations: it systematically rises from barely 10% in the beginning of glacials to about 60% during glacial maximums (Fig. 4, middle), indicating that marine isotope values cannot be linearly converted into sea level (see Supplementary Information). The latter translates into a mean ocean isotope increase of 1.05‰ during the LGM; this matches estimates based on $\delta^{18}O$ of relict pore water of 1.05 ± 0.2‰ (refs 8, 22) very well.

The main strength of our method is that it yields long and mutually consistent records of surface air temperature, ice volume and global sea level by separating the ice-sheet and deep-water parts of the marine $\delta^{18}O$ signal. This allows us to precisely compare the timing of the fluctuations of these climate variables. As an example, our results show that temperature changes (atmosphere and ocean) lead changes in Northern Hemisphere ice volume, which are dominated by the North American ice sheets, particularly during glacial inception stages but also during terminations[5]. Future analyses may yield clues about causes and effects concerning ice age climatic fluctuations.

METHODS

Inverse procedure. The inverse procedure (observation-constrained forward modelling) centres around the calculation of surface air temperature (continental mean over 40° − 80° N) relative to the present (ΔT) based on the difference between the modelled marine isotope value ($I_m(t)$) and the observed value δt (= 0.1 kyr) later ($I_o(t+\delta t)$): $\Delta T = \overline{\Delta T_b} + c[I_m(t) - I_o(t+\delta t)]$ The first term on the right-hand side represents the average ΔT over the last b kyr that precede time t, while the parameter c in the second term determines how quickly ΔT responds to fluctuations in the marine isotope record. Optimal values of b (= 2 kyr) and c (= 160 °C ‰$^{-1}$) were obtained by minimizing the sum of the squared differences between modelled and observed oceanic $\delta^{18}O$ over the 1,070-kyr period. Using these values, the difference always remained less than 0.25% of the $\delta^{18}O$ signal.

The procedure is then as follows (see also Fig. 1): if the modelled isotope value is smaller than the value of I_o 0.1 kyr later, temperatures should drop because (1) the model ocean must increase its relative heavy-isotope content through the build-up of ice sheets (where light isotopes are preferentially stored), and (2) the modelled uptake of ^{18}O in the carbonate shells of foraminifera should increase (obviously, warming occurs for $I_m > I_o$). The new marine isotope value is subsequently evaluated from the updated atmospheric air temperature according to: $V_o I_m - (V_o I_m)_{PD} = -\lambda V_i I_i - \gamma \Delta T_o$, where V_o and V_i represent ocean and ice volume (in km^3 water equivalent) respectively (PD refers to present-day conditions), I_i is the ice sheet isotope content (in ‰), ΔT_o is the deep-water temperature anomaly from present (in °C) and λ and γ are empirical parameters (discussed below). Both the ice-sheet and deep-water terms on the right-hand-side become larger when temperatures drop (I_i and ΔT_o have negative values). Hence, the simulated marine isotope value (I_m) increases as required. Its new value is then passed on to the following time step to evaluate the next change in air temperature. Starting at 1,070 kyr BP, this procedure runs to the present with 0.1-kyr steps.

Ice-sheet and deep-water models. The physical part of the method consists of two components: (1) the ice-sheet model, including an isotope budget, and (2) the atmosphere–deep-water temperature coupling. The first involves the ocean's changing isotopic composition, which depends on the amount of (light) isotopes stored in continental ice ($V_i I_i$). To simulate the evolution of the Northern Hemisphere ice sheets (excluding Greenland[5]), we used a detailed three-dimensional thermomechanical ice sheet + ice shelf + bedrock model to solve the prognostic equations for ice thickness, ice temperature and bedrock height[6,12]. Changes in ice-sheet isotope budget were explicitly calculated, which has rarely been attempted before[23,24]. It is assumed that spatial and temporal $\delta^{18}O$ variations in accumulating snow depend on surface air temperature[25,26]. Once part of the ice sheet, the $\delta^{18}O$ content—a passive tracer—is transported downslope with the vertically averaged ice velocity. The majority of the ice-sheet part of the marine oxygen isotope changes can be attributed to the Northern

© 2005 Nature Publishing Group

Hemisphere ice sheets, but not all. On the basis of interglacial–glacial differences in isotope content and volume of the Antarctic and Greenland ice sheets[8,27] we estimate that together they contribute 5% to global oceanic isotope variations (hence $\lambda = 1.05$), and 15% to sea-level variations[6].

The second model component relates to the dependence of benthic $\delta^{18}O$ on deep-water temperature (ΔT_o). To take this into account, we needed to incorporate a coupling between mean deep-water temperature and Northern Hemisphere surface air temperature, which are related through vertical mixing and deep-water formation. Several proxy-based deep-water temperature reconstructions show that bottom-water temperatures were several degrees lower during glacials than during interglacials[8–10]. Moreover, long-term (glacial–interglacial) deep-water and surface temperature proxy variations exhibit sufficient coherence to justify using a simple relation between them. Hence, we parameterized the dependence of deep-water temperature (δT_d) on the 3-kyr mean Northern Hemisphere midlatitude surface air temperature (δT_a)—which are both deviations from the present—by using a idealized climate–ocean model[28]: $\delta T_d = 0.2\delta T_a$. This effectively introduces a lag of 2–5 kyr between δT_d and δT_a. An empirical linear relation[29] between deep-water temperature and $\delta^{18}O$ with a slope of $-0.28‰\,°C^{-1}$ (ref. 8) then quantifies the deep-sea part of the oxygen isotope signal (hence $\gamma = 0.28‰\,°C^{-1}$).

Estimation of the uncertainty. Several sensitivity tests were carried out to quantify the uncertainty associated with the method (error envelopes in Figs 2 and 3). These are based on the uncertainty in key model/input parameters[12]: the input oxygen isotope record (reflecting the standard error of the stack[11], a measure of local deep-water mass variability[5,8]), changes in seasonality of the temperature forcing[12], the temperature–$\delta^{18}O$ relationship in precipitation[25] (related to the temporally variable and poorly quantified Dole effect[30], among other things), the atmosphere–deep-water temperature relationship, and the isotopic contributions from Antarctica and Greenland.

Received 7 March; accepted 29 June 2005.

1. Waelbroeck, C. *et al.* Sea-level and deep water temperature changes derived from benthic foraminifera isotopic records. *Quat. Sci. Rev.* **21,** 295–305 (2002).
2. Lambeck, K., Esat, T. M. & Potter, E. Links between climate and sea levels for the past three million years. *Nature* **419,** 199–206 (2002).
3. Shackleton, N. J. The 100,000-year ice-age cycle identified and found to lag temperature, carbon dioxide, and orbital eccentricity. *Science* **289,** 1897–1902 (2000).
4. Paillard, D. Glacial cycles: toward a new paradigm. *Rev. Geophys.* **39,** 325–346 (2001).
5. Lea, D. W., Martin, P. A., Pak, D. K. & Sperbo, H. J. Reconstructing a 350-kyr history of sea level using planktonic Mg/Ca and oxygen isotope records from a Cocos Ridge core. *Quat. Sci. Rev.* **21,** 283–293 (2002).
6. Bintanja, R., van de Wal, R. S. W. & Oerlemans, J. Global ice volume variations through the last glacial cycle simulated by a 3-D ice-dynamical model. *Quat. Int.* **95–96,** 11–23 (2002).
7. Imbrie, J., *et al.* in *Milankovitch and Climate* (eds Berger, A. L. & Reidel, D.) 269–305 (Kluwer Academic, Boston, 1984).
8. Duplessy, J.-C., Labeyrie, L. & Waelbroeck, C. Constraints on the ocean oxygen isotopic enrichment between the Last Glacial Maximum and the Holocene: paleoceanographic implications. *Quat. Sci. Rev.* **21,** 315–330 (2002).
9. Cutler, K. B. *et al.* Rapid sea-level fall and deep-ocean temperature change since the last interglacial period. *Earth Planet. Sci. Lett.* **206,** 253–271 (2003).
10. Dwyer, G. S. *et al.* North Atlantic deepwater temperature change during late Pliocene and late Quaternary climatic cycles. *Science* **270,** 1347–1351 (1995).
11. Lisiecki, L. E. & Raymo, M. E. A Pliocene-Pleistocene stack of 57 globally distributed benthic $\delta^{18}O$ records. *Paleoceanography* **20,** doi:10.1029/2004PA001071 (2005).
12. Bintanja, R., van de Wal, R. S. W. & Oerlemans, J. A new method to estimate ice age temperatures. *Clim. Dyn.* **24,** 197–211 (2005).
13. Kageyama, M. *et al.* The last glacial maximum climate over Europe and western Siberia: a PMIP comparison between models and data. *Clim. Dyn.* **17,** 23–43 (2001).
14. EPICA community members, Eight glacial cycles from an Antarctic ice core. *Nature* **429,** 623–628 (2004).
15. North Greenland Ice Core Project members, High-resolution record of Northern Hemisphere climate extending into the last interglacial period. *Nature* **431,** 147–151 (2004).
16. Siddall, M. *et al.* Sea-level fluctuations during the last glacial cycle. *Nature* **423,** 853–858 (2003).
17. Lambeck, K. & Chappell, J. Sea level change through the last glacial cycle. *Science* **292,** 679–686 (2001).
18. Clark, P. U., Alley, R. B. & Pollard, D. Northern hemisphere ice sheet influences on global climate change. *Science* **286,** 1104–1111 (1999).
19. Tarasov, L. & Peltier, W. R. Terminating the 100 kyr ice age cycle. *J. Geophys. Res.* **102,** 21665–21693 (1997).
20. Svendsen, J. I. *et al.* Late quaternary ice sheet history of northern Eurasia. *Quat. Sci. Rev.* **23,** 1229–1271 (2004).
21. Cortijo, E. *et al.* Eemian cooling in the Norwegian Sea and North Atlantic ocean preceding continental ice sheet growth. *Nature* **372,** 446–449 (1994).
22. Schragg, D. P., Hampt, G. & Murray, D. W. Pore fluid constraints on the temperature and oxygen isotope composition of the glacial ocean. *Science* **372,** 1930–1932 (1996).
23. Mix, A. C. & Ruddiman, W. F. Oxygen-isotope analyses and Pleistocene ice volumes. *Quat. Res.* **21,** 1–20 (1984).
24. Clarke, G. K. C. & Marshall, S. J. Isotopic balance of the Greenland Ice sheet: modelled concentrations of water isotopes from 30,000 BP to present. *Quat. Sci. Rev.* **21,** 419–430 (2002).
25. Cuffey, K. M. *et al.* Large Arctic temperature change at the Wisconsin-Holocene glacial transition. *Science* **270,** 455–458 (1995).
26. Fricke, H. C. & O'Neil, J. R. The correlation between $^{18}O/^{16}O$ ratios of meteoric water and surface temperature: its use in investigating terrestrial climate change over geologic time. *Earth Planet. Sci. Lett.* **170,** 181–196 (1999).
27. Huybrechts, P. Sea-level changes at the LGM from ice-dynamic reconstructions of the Greenland and Antarctic ice sheets during glacial cycles. *Quat. Sci. Rev.* **21,** 203–231 (2002).
28. Bintanja, R. & Oerlemans, J. The effect of reduced ocean overturning on the climate of the last glacial maximum. *Clim. Dyn.* **12,** 523–533 (1996).
29. Shackleton, N. J. *Les Méthodes Quantitatives d'étude des Variations du Climat au Cours du Pleistocène* CNRS, Gif sur Yvette, [in English] 203–209 (1974).
30. Jouzel, J., Hoffmann, G., Parrenin, F. & Waelbroeck, C. Atmospheric oxygen 18 and sea-level changes. *Quat. Sci. Rev.* **21,** 307–314 (2002).

Supplementary Information is linked to the online version of the paper at www.nature.com/nature.

Acknowledgements Financial support was provided by the Netherlands Organisation of Scientific Research (NWO), in the framework of the SPINOZA award of J. Oerlemans. Constructive remarks were provided by M. Siddall and D. Dahl-Jensen.

Author Information Reprints and permissions information is available at npg.nature.com/reprintsandpermissions. The authors declare no competing financial interests. Correspondence and requests for materials should be addressed to R.B. (R.Bintanja@phys.uu.nl).

© 2005 Nature Publishing Group